

Kinetics and Mechanism of the Oxidation of $[\text{Fe}(\text{CN})_6]^{4-}$ to $[\text{Fe}(\text{CN})_6]^{3-}$, Induced by the Reaction between Cu^{2+} and I^- in Aqueous Solution. Oxidation Reaction by a Radical Anion $\text{I}_2^{\cdot -}$

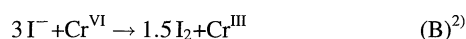
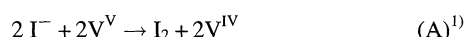
Masaru Kimura,* Yuko Shiota, Shinobu Kishi, and Keiichi Tsukahara*

Department of Chemistry, Faculty of Science, Nara Women's University, Nara 630-8506

(Received January 25, 1999)

The hexacyanoferrate(II) ion ($[\text{Fe}(\text{CN})_6]^{4-}$) was rapidly oxidized to $[\text{Fe}(\text{CN})_6]^{3-}$ by a radical anion, $\text{I}_2^{\cdot -}$, which was formed by a reaction between the copper(II) ion and the iodide ion. The oxidation reaction was accelerated by increasing the pH. Under the conditions of lower pH's, the $[\text{Fe}(\text{CN})_6]^{3-}$ acted as a retarder to the oxidation reaction. The mechanisms for such reactions are discussed in terms of accounting for the obtained results.

A trace amount of metal ion, such as copper(II), plays an important role in catalytic cycles of a number of redox reactions. Our recent studies^{1,2)} have indicated that, when a copper(II) solution in 10^{-8} — 10^{-5} M ($\text{M} = \text{mol dm}^{-3}$) was mixed with an iodide solution of 0.10 M, after a rapid formation of iodine (and/or triiodide), the iodine concentration remained constant without precipitations of CuI . After such an iodine formation had occurred, when an oxidizing reagent such as Cr^{VI} or V^{V} was added into the reacted mixture, the iodine concentration began to increase, indicating the reformation of I_2 (and/or I_3^-) by a catalytic redox cycle of $\text{Cu}(\text{II})/\text{Cu}(\text{I})$, and the formed iodine-concentration reached the stoichiometric concentration for the added oxidizing reagent (see the following equations with (2) and (3) in Fig. 1):



On the contrary, when the $[\text{Fe}(\text{CN})_6]^{3-}$ ion was added into the same mixture, the iodine-formation behavior was extremely different from the cases in any other oxidants, indicating a slight decrease of I_3^- in the case of the relatively lower concentrations of the added $[\text{Fe}(\text{CN})_6]^{3-}$, and that much smaller formations of I_3^- than the added $[\text{Fe}(\text{CN})_6]^{3-}$ concentration were found in the case of the relatively higher concentrations of $[\text{Fe}(\text{CN})_6]^{3-}$ (refer to (4a) and (4b) in Fig. 1). Further, it appeared that there are, in plots of $[\text{I}_3^-]_{\text{formed}}$ vs. t , some fluctuations, like oscillating reactions, after adding $[\text{Fe}(\text{CN})_6]^{3-}$ (see (4a) and (4b) in Fig. 1). Instead, the addition of $[\text{Fe}(\text{CN})_6]^{4-}$ led to a stoichiometric decrease in the iodine concentration along with a stoichiometric increase in $[\text{Fe}(\text{CN})_6]^{3-}$ under suitable conditions of pH (see (5) in Fig. 1). This is very novel and interesting for a discussion of the mechanisms to account for the obtained results, which would contain a new catalytic cycle due to the

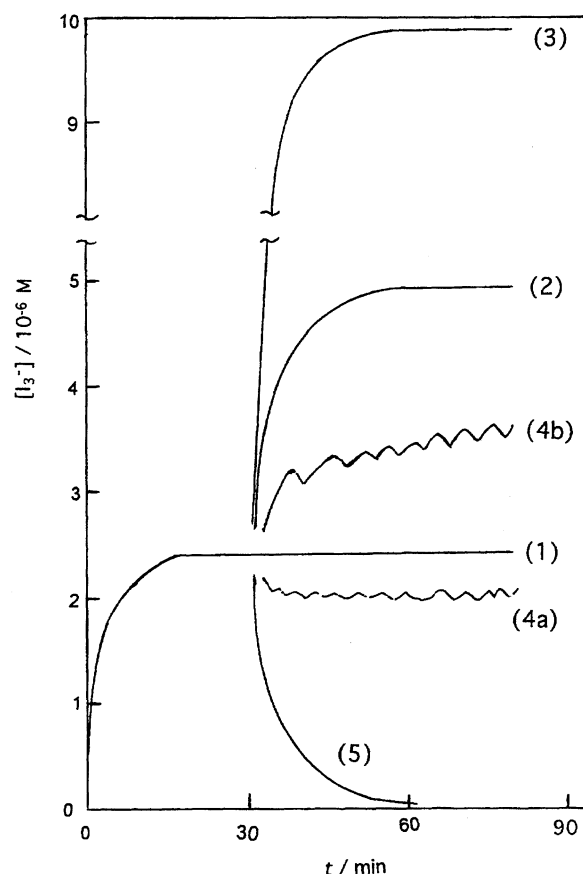


Fig. 1. Profile of the copper(II)-catalyzed reactions.

Curve (1) indicates the case of the I_3^- formation by the reaction between 0.10 M I^- and 6.0×10^{-6} M Cu^{2+} at pH 3.5 but (4b). Curves (2), (3), (4a), and (5) indicate the cases that 5.0×10^{-6} M of V^{V} , Cr^{VI} , $[\text{Fe}(\text{CN})_6]^{3-}$, or $[\text{Fe}(\text{CN})_6]^{4-}$ was added at 30 min into the reacted solution of (1), respectively, and the curve (4b), the case that $[\text{Fe}(\text{CN})_6]^{3-}$ of 2.0×10^{-5} M was added at pH 1.9.

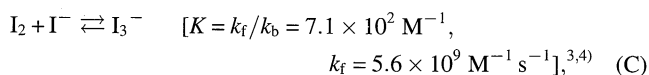
Cu^{II} and Cu^I ions with I^-/I_3^- .

Experimental

Chemicals. Potassium hexacyanoferrate(II) ($K_4[Fe(CN)_6] \cdot 3H_2O$), potassium hexacyanoferrate(III) ($K_3[Fe(CN)_6]$), copper(II) sulfate ($CuSO_4 \cdot 5H_2O$), potassium iodide (KI), iodine (I_2), and the other chemicals were of guaranteed grade from Wako Pure Chemical Industries, Ltd.

Procedure. The reaction was started by mixing an iodide solution into a copper(II) solution without or with $[Fe(CN)_6]^{4-}$ or $[Fe(CN)_6]^{3-}$; in some runs the ferrate solution was added at various times after having mixed an iodide solution with the copper(II) solution. The formed (or reduced) I_3^- concentrations were determined by measuring the absorbance of I_3^- at 350 nm using a Shimadzu UV-150-02 spectrophotometer. The temperature of the reaction solution was controlled to $(25.0 \pm 0.1)^\circ C$. The dissolved oxygen was removed by bubbling N_2 -gas through the solution; after starting the reaction, N_2 -gas was continuously supplied to the solution surface during the reaction. Aliquot solutions were taken out at appropriate time intervals in order to measure the absorbance of the formed I_3^- .

The iodine and triiodide in the presence of the iodide ion are in the following equilibrium:



Thus, the concentrations of I_3^- were actually equivalent to those of I_2 under the conditions of large excess of I^- . The molar absorption coefficient of I_3^- was 3.8×10^4 and $2.5 \times 10^4 \text{ M}^{-1} \text{ cm}^{-1}$ at 288 and 350 nm, respectively,⁵⁾ and thus, the absorbance of I_3^- at 350 nm was used to follow kinetic runs and to measure the formed (or decreased) I_3^- concentrations, where the molar absorption coefficients at 350 nm for $[Fe(CN)_6]^{4-}$ and $[Fe(CN)_6]^{3-}$ were 1.6×10^2 and $3.3 \times 10^2 \text{ M}^{-1} \text{ cm}^{-1}$, respectively, which are much smaller than $2.5 \times 10^4 \text{ M}^{-1} \text{ cm}^{-1}$ for I_3^- . Therefore, the obtained absorbance at 350 nm could be assumed as that for the I_3^- species. The maximum absorption wavelength for $[Fe(CN)_6]^{3-}$ was 420 nm ($\epsilon_{420} = 1.0 \times 10^3 \text{ M}^{-1} \text{ cm}^{-1}$), and the absorption at 420 nm for $[Fe(CN)_6]^{4-}$ was negligible. Thus, the $[Fe(CN)_6]^{3-}$ concentrations in Table 1 and Fig. 6, inset were determined by using the following equation:

$$A_{420} = \{\epsilon_1 [[Fe(CN)_6]^{3-}] + \epsilon_2 [I_3^-]\} I, \quad (D)$$

where A_{420} indicates the absorbance at 420 nm observed by using $I = 1 \text{ cm}$ for the photo-cell length; $\epsilon_1 (= 1.0 \times 10^3 \text{ M}^{-1} \text{ cm}^{-1})$ and $\epsilon_2 (= 3.0 \times 10^3 \text{ M}^{-1} \text{ cm}^{-1})$ mean the molar absorption coefficients at 420 nm for $[Fe(CN)_6]^{3-}$ and I_3^- , respectively.

Results

Oxidation Reactions by $[Fe(CN)_6]^{3-}$. When $[Fe(CN)_6]^{3-}$ was added into a solution containing I_3^- formed by the reaction between Cu^{2+} and I^- , the I_3^- concentration decreased slightly and then remained almost constant under the conditions of the relatively low concentrations of $[Fe(CN)_6]^{3-}$, and began to increase rapidly and then gradually under the conditions of the relatively higher concentrations of $[Fe(CN)_6]^{3-}$. In any case, some fluctuations, like oscillations in the plots, were observed (see plots after 30 min in Figs. 2 and 5A). On the other hand, when $[Fe(CN)_6]^{3-}$ together with Cu^{2+} was added into the I^- solution, the I_3^- formation occurred rapidly once and then became rather constant at almost the same time as in the case without adding $[Fe(CN)_6]^{3-}$ (compare ● to the other plots at $t \leq 20 \text{ min}$ in Fig. 2). In the case without adding copper(II) ion, the $[Fe(CN)_6]^{3-}$ oxidized I^- to iodine at a much slower rate than in the case of having added Cu^{2+} (compare inset to the plots at $t \leq 20 \text{ min}$ in Fig. 2 in which there is a rapid formation of I_3^- during $t = 0-2 \text{ min}$). This indicates that the CuI , which was formed by the reaction between I^- and Cu^{2+} , was rapidly oxidized to CuI^+ by $[Fe(CN)_6]^{3-}$ (refer to Eq. 8), and that the redox cycle of CuI/CuI^+ accelerated the oxidation reaction of I^- by $[Fe(CN)_6]^{3-}$. It is to be noted that the plots (○) in Fig. 2, which are less the concentrations of the added $[Fe(CN)_6]^{3-}$, were much larger than Δ at $t \leq 20 \text{ min}$, and were slightly larger than (or almost equivalent to) Δ at $t > 30 \text{ min}$, indicating that the formation rate of I_3^- by $[Fe(CN)_6]^{3-}$ competes with its reduction rate by $[Fe(CN)_6]^{4-}$.

Oxidation Reactions of $[Fe(CN)_6]^{4-}$ to $[Fe(CN)_6]^{3-}$. When $[Fe(CN)_6]^{4-}$ instead of $[Fe(CN)_6]^{3-}$ in Fig. 2 was used, the I_3^- concentration greatly decreased, and then be-

Table 1. Stoichiometry^{a)}

t/min	$[I_3^-]_{\text{decreased}}/10^{-6} \text{ M}$	$[Fe(CN)_6]^{3-}_{\text{formed}}/10^{-6} \text{ M}$	$[Fe(CN)_6]^{3-}_{\text{formed}}/[I_3^-]_{\text{decreased}}$
31.5	4.90	9.60	1.9 ₆
32.0	5.10	10.1	1.9 ₈
32.5	5.18	10.4	2.0 ₁
33.0	5.24	10.4	1.9 ₈
33.5	5.26	10.4	1.9 ₈
34.0	5.26	10.5	2.0 ₀
34.5	5.26	10.5	2.0 ₀
35.0	5.26	10.5	2.0 ₀
37.0	5.26	10.5	2.0 ₀
40.0	5.26	10.5	2.0 ₀
45.0	5.20	10.4	2.0 ₀
50.0	5.26	10.2	2.0 ₀
60.0	5.26	10.5	2.0 ₀
			Av. 2.0

a) $1.05 \times 10^{-5} \text{ M}$ $[Fe(CN)_6]^{4-}$ was added to the reacted mixture at 30.0 min after a $CuSO_4$ solution ($2.0 \times 10^{-5} \text{ M}$) was mixed with 0.10 M KI solution under conditions of pH 4.0, N_2 -saturated, and $25^\circ C$.

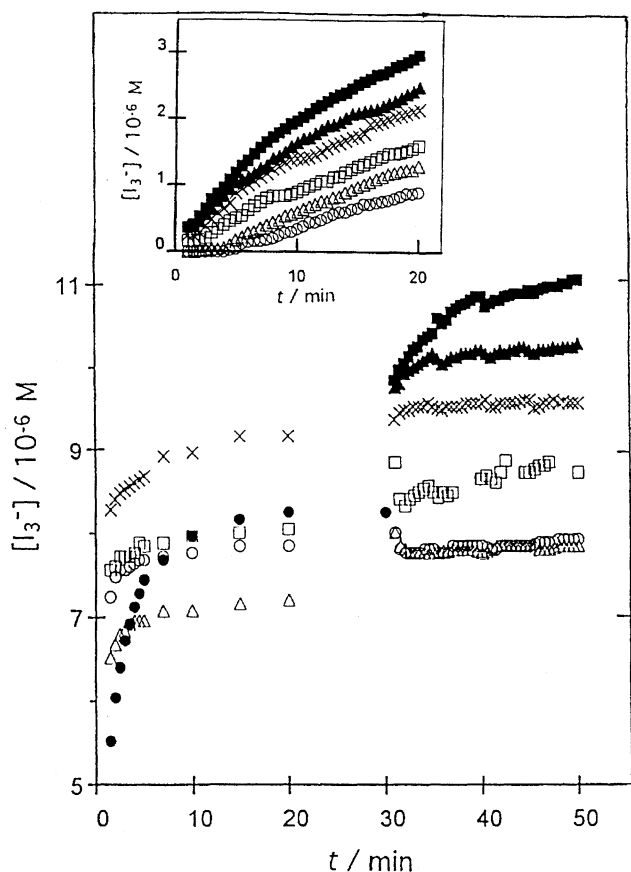


Fig. 2. Reactions with $[\text{Fe}(\text{CN})_6]^{3-}$ at 25.0°C , pH 1.9 (0.010 M H_2SO_4), and N_2 -sat.

Plots of \bullet indicate results in the reaction between 0.10 M I^- and $2.0 \times 10^{-5}\text{ M Cu}^{2+}$. $[\text{Fe}(\text{CN})_6]^{3-}$ was mixed at $t = 0$ or 30 min with the reacted solution in the plots \bullet . Plots \circ , \triangle , \square , \times , \blacktriangle , and \blacksquare indicate $[\text{Fe}(\text{CN})_6]^{3-}_{\text{added}}/10^{-5}\text{ M} = 1.0, 1.2, 1.4, 1.6, 1.8, \text{ and } 2.0$, respectively, and the insert figure, the I_3^- formation by the oxidation of I^- by $[\text{Fe}(\text{CN})_6]^{3-}$ without adding the copper(II) ion.

came constant at about 20 min after adding the $\text{Fe}(\text{II})$ complex ion (Fig. 3A). The decreased concentrations of I_3^- at $t \geq 50$ min in Fig. 3A were proportional to those of the added $[\text{Fe}(\text{CN})_6]^{4-}$ (see Fig. 3A). Further, as can be seen from Table 1, the decreased concentrations of I_3^- were half of the formed ones of $[\text{Fe}(\text{CN})_6]^{3-}$, indicating the stoichiometric equation of $\text{I}_3^- + 2[\text{Fe}(\text{CN})_6]^{4-} \rightarrow 3\text{I}^- + 2[\text{Fe}(\text{CN})_6]^{3-}$, which corresponds to the backward reaction in Eq. 10. On the other hand, in the case of no addition of copper(II), $[\text{Fe}(\text{CN})_6]^{4-}$ reduced I_3^- to I^- at a much slower rate than that in the presence of the copper(II) ion (compare A to B in Fig. 3). This indicates that the oxidation reaction of $[\text{Fe}(\text{CN})_6]^{4-}$ by I_3^- was catalytically accelerated by the redox cycle of CuI^+/CuI .

Effect of the Added Copper(II) Concentrations. As can be seen from Fig. 4, when the concentrations of the added copper(II) decreased, the rates for not only the formation of I_3^- before adding $[\text{Fe}(\text{CN})_6]^{4-}$, but also its decomposition after having added $[\text{Fe}(\text{CN})_6]^{4-}$, decreased greatly, and the initial rate ($V_i = \Delta[\text{I}_3^-]_i/\Delta t$) of the I_3^- decomposition after having added $[\text{Fe}(\text{CN})_6]^{4-}$ was proportional to the I_3^- con-

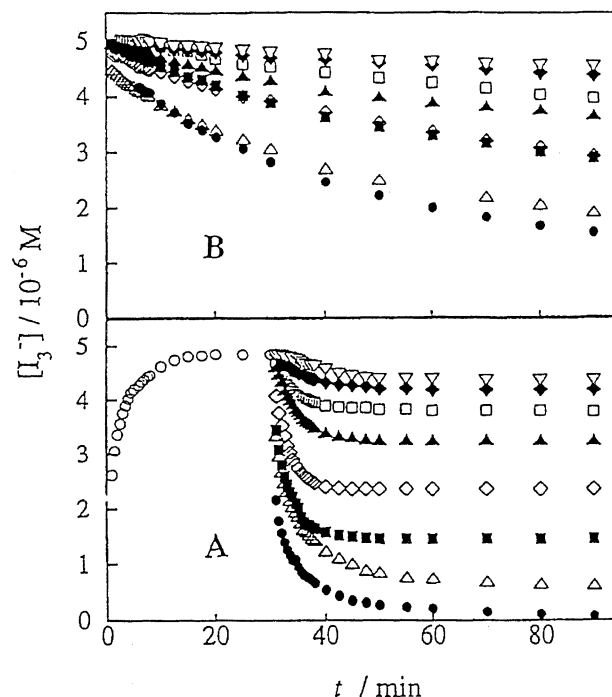


Fig. 3. Reactions with $[\text{Fe}(\text{CN})_6]^{4-}$ at 25.0°C , pH 3.5 (0.050 M CH_3COOH –0.0050 M CH_3COONa), and N_2 -sat.

A: Plots \circ indicate the I_3^- formation by the reaction of Cu^{2+} ($1.2 \times 10^{-5}\text{ M}$) with I^- (0.10 M). $[\text{Fe}(\text{CN})_6]^{4-}$ was added at $t = 30$ min to a reacted solution of Cu^{2+} with I^- (i.e., the plots \circ), where $[\text{Fe}(\text{CN})_6]^{4-}_{\text{added}}/10^{-6}\text{ M} = 0.50, 1.0, 2.0, 3.0, 5.0, 6.0, 8.0, \text{ and } 10$ for the plots $\nabla, \blacklozenge, \square, \blacktriangle, \diamond, \blacksquare, \triangle, \text{ and } \bullet$, respectively.

B: $[\text{Fe}(\text{CN})_6]^{4-}$ was added into a solution of I_3^- ($5.0 \times 10^{-6}\text{ M}$) I_2 with 0.10 M KI in the absence of the copper(II) ion. All other conditions with symbols are the same as those in A.

centrations at the time of having added it (see Fig. 4, inset).

Effect of pH. Figure 5A indicates that the rate in the catalyzed reaction with $[\text{Fe}(\text{CN})_6]^{3-}$ increased along with decreasing pH. On the contrary, the rate in a catalyzed reaction with $[\text{Fe}(\text{CN})_6]^{4-}$ decreased with decreasing pH, and did not reach the stoichiometric concentration (see Fig. 5B). Further, as can be seen from plots \blacksquare and \blacktriangle in the lower pH's (Fig. 5B), the I_3^- concentrations decreased once and then began to increase slightly, indicating the existence of a competitive reaction in the reduction and formation reactions of I_3^- .

Evidence of Oxidation of $[\text{Fe}(\text{CN})_6]^{4-}$ by $\text{I}_2^{\cdot-}$. As can be seen from Fig. 6, when $[\text{Fe}(\text{CN})_6]^{4-}$ was added into a HNO_2 solution containing O_2 with I^- , in which it has been known⁶⁾ to produce I_3^- via the preformation of $\text{I}_2^{\cdot-}$ by the reaction $2\text{I}_2^{\cdot-} \rightleftharpoons \text{I}_3^- + \text{I}^-$ (Eq. 4), I_3^- formation for the initial periods at $t \leq 3$ min was greatly retarded by $[\text{Fe}(\text{CN})_6]^{4-}$, and then began to increase at the same rate as in the case of having added $[\text{Fe}(\text{CN})_6]^{3-}$. This indicates that almost all of the added $[\text{Fe}(\text{CN})_6]^{4-}$ was rapidly oxidized during $t \leq 3$ min to $[\text{Fe}(\text{CN})_6]^{3-}$ by $\text{I}_2^{\cdot-}$ which was produced by the reaction between HNO_2 and I^- together with O_2 .

Since the oxidation reactions of the oxalate ion by $\text{I}_2^{\cdot-}$

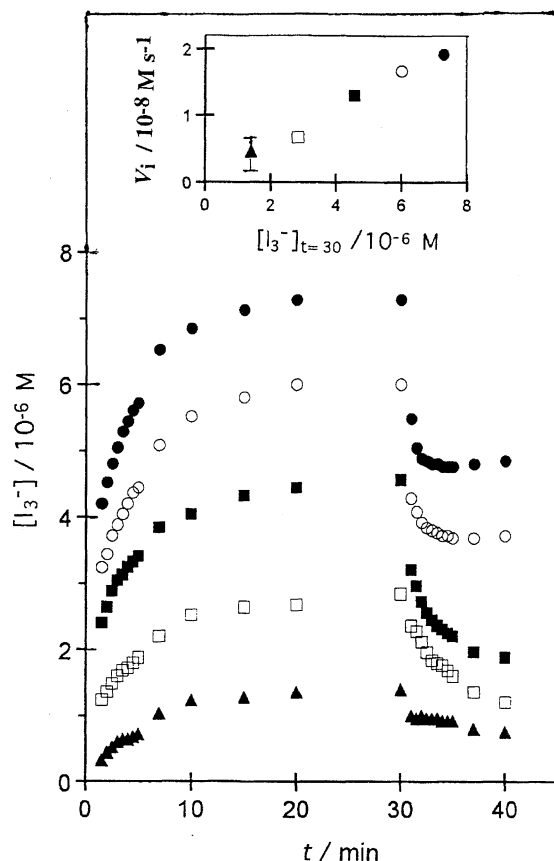


Fig. 4. Effect of the copper(II) concentrations. Plots \bullet , \circ , \blacksquare , \square , and \blacktriangle indicate the added copper(II) concentrations of 1.8×10^{-5} , 1.5×10^{-5} , 1.1×10^{-5} , 7.3×10^{-6} , and $3.5 \times 10^{-6} \text{ M}$, respectively. Inset is the plot of V_i ($= \Delta[I_3^-]_i / \Delta t$ at $t \geq 30 \text{ min}$) vs. $[I_3^-]_{t=30}$. The other conditions are $5.0 \times 10^{-6} \text{ M}$ $[\text{Fe}(\text{CN})_6]^{4-}$, pH 4.0 (0.050 M CH_3COOH –0.010 M CH_3COONa), N_2 -sat., and 25°C .

have been known,⁵⁾ the retardation effect upon the oxalate addition on the I_3^- formation in the HNO_2/I^- reaction system is also presented together with the retardation effect by $[\text{Fe}(\text{CN})_6]^{4-}$ in Fig. 6. Comparing the retardation effects by $[\text{Fe}(\text{CN})_6]^{4-}$ and oxalate in Fig. 6, the former was over 10^3 -fold more effective than the latter. Further, we confirmed the oxidation reaction by $I_2^{\cdot-}$ through determining the $[\text{Fe}(\text{CN})_6]^{3-}$ concentration (see Table 1 and inset in Fig. 6). As can be seen from Fig. 6, inset, all of the added $[\text{Fe}(\text{CN})_6]^{4-}$ became $[\text{Fe}(\text{CN})_6]^{3-}$ at $t \leq 3 \text{ min}$; the decrease in the concentration of $[\text{Fe}(\text{CN})_6]^{3-}$ after about 4 min is thought to be due to the reduction of $[\text{Fe}(\text{CN})_6]^{3-}$ by I^- (compare plots \bullet with \blacktriangle in Fig. 6, inset). Similarly, as in Fig. 6, Table 1 indicates the oxidation of $[\text{Fe}(\text{CN})_6]^{4-}$ to $[\text{Fe}(\text{CN})_6]^{3-}$ by the anion radical $I_2^{\cdot-}$, which is present in the $\text{Cu}^{2+}/\text{I}^-$ mixture. It is to be noted that the $[\text{Fe}(\text{CN})_6]^{3-}$ once formed did not decrease, as shown in Table 1, being different from the case in Fig. 6, and that such a behavior as that in the case of Table 1 is related to the reaction mechanism, being composed of several competing reactions, including the CuI/CuI^+ cycle (v.i.).

Retardation Effect by Radical Scavengers. It is

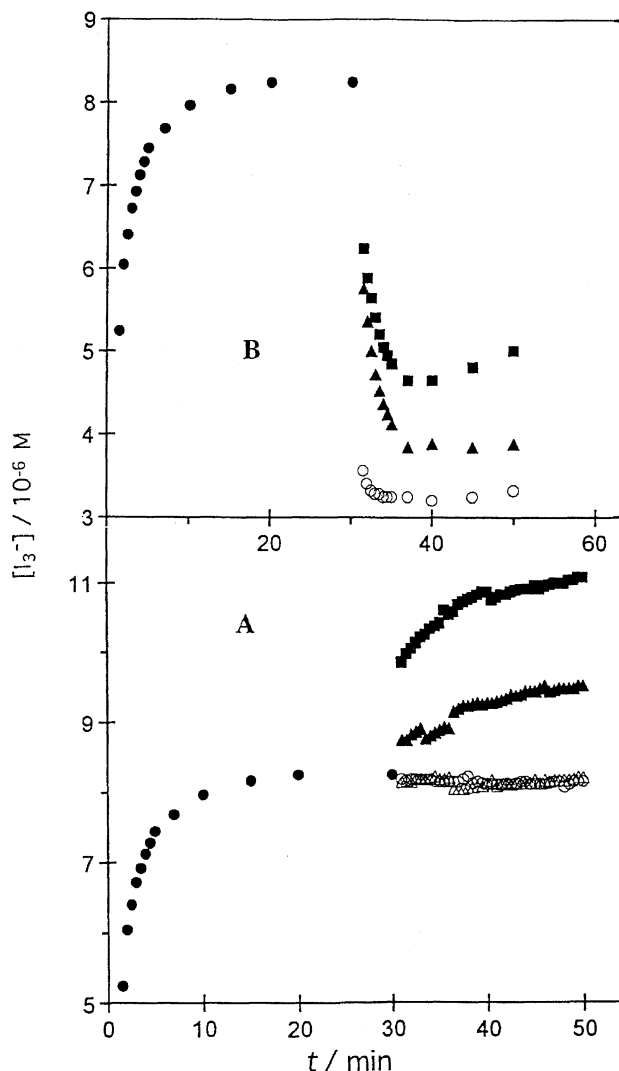


Fig. 5. pH Effects. Plots \bullet indicate the I_3^- formation by the reaction of Cu^{2+} ($2.0 \times 10^{-5} \text{ M}$) with I^- (0.10 M) under conditions of N_2 -saturated at 25.0°C .

A: pH effect of the case that $2.0 \times 10^{-5} \text{ M}$ $[\text{Fe}(\text{CN})_6]^{3-}$ was added at 30 min into the reacted solution in the plots \bullet , where pH was 1.9, 2.4, 3.0, and 3.8 for the plots \blacksquare , \blacktriangle , \triangle , and \circ , respectively.

B: pH effect of the case that $1.0 \times 10^{-5} \text{ M}$ $[\text{Fe}(\text{CN})_6]^{4-}$ was added at 30 min into the reacted solution in the plots \bullet , where the pH values were 1.9, 2.4, and 4.0 for the plots \blacksquare , \blacktriangle , and \circ , respectively.

known that aminocarboxylates containing EDTA^{7,8)} as well as oxalate⁵⁾ can be easily oxidized by the radical $I_2^{\cdot-}$. Thus, we added either acrylonitrile, acrylamide, oxalate, or EDTA as a radical scavenger into the reacted solution of Cu^{2+} with I^- , and found that any one of these led to a large decrease of I_3^- (see Fig. 7). Both results shown in Figs. 6 and 7 mean the presence of $I_2^{\cdot-}$ in an equilibrium state, such as Eq. 5. The strength order in the retardation effect, i.e., the reaction rate of $I_2^{\cdot-}$ with retarders was $[\text{Fe}(\text{CN})_6]^{4-} \gg \text{oxalate}$ from Fig. 6, and $[\text{Fe}(\text{CN})_6]^{4-} \gg \text{EDTA} > \text{oxalate} > \text{acrylamide} > \text{acrylonitrile}$ from Fig. 7.

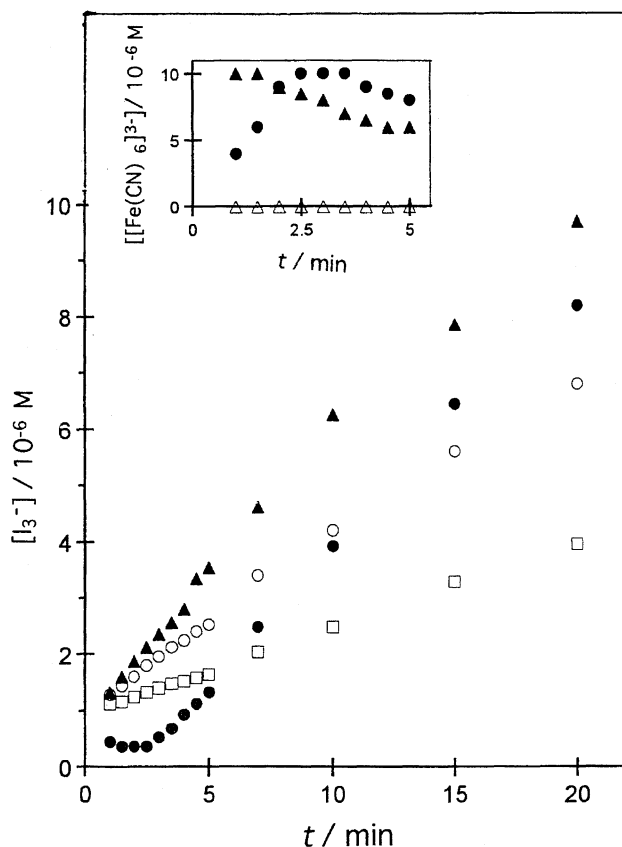


Fig. 6. Evidence of the oxidation reaction of $[\text{Fe}(\text{CN})_6]^{4-}$ to $[\text{Fe}(\text{CN})_6]^{3-}$ by I_2^- .

The plots \circ indicate the case that NaNO_2 (1.0×10^{-5} M) was added into a KI solution (0.10 M) under conditions of the air-saturated at pH 4.0 (0.050 M CH_3COOH –0.010 M CH_3COONa) and 25 °C. Plots \blacktriangle , \bullet , and \square indicate that 1.0×10^{-5} M $[\text{Fe}(\text{CN})_6]^{3-}$, 1.0×10^{-5} M $[\text{Fe}(\text{CN})_6]^{4-}$, or 0.010 M $\text{C}_2\text{O}_4^{2-}$ together with NaNO_2 was mixed with the KI solution under the same conditions as those in plots \circ . The plots \triangle in inset indicate the case that 1.0×10^{-5} M $[\text{Fe}(\text{CN})_6]^{4-}$ with 0.10 M KCl was mixed with NaNO_2 (1.0×10^{-5} M) under the same conditions as those in the other plots.

Discussion

Figures 2 and 3 indicate that both reactions $[\text{Fe}(\text{CN})_6]^{3-}$ with I^- and $[\text{Fe}(\text{CN})_6]^{4-}$ with I_3^- are greatly accelerated by the catalytic redox cycle of $\text{Cu}^{\text{II}}/\text{Cu}^{\text{I}}$, and thus we can assume the following mechanism of reaction:

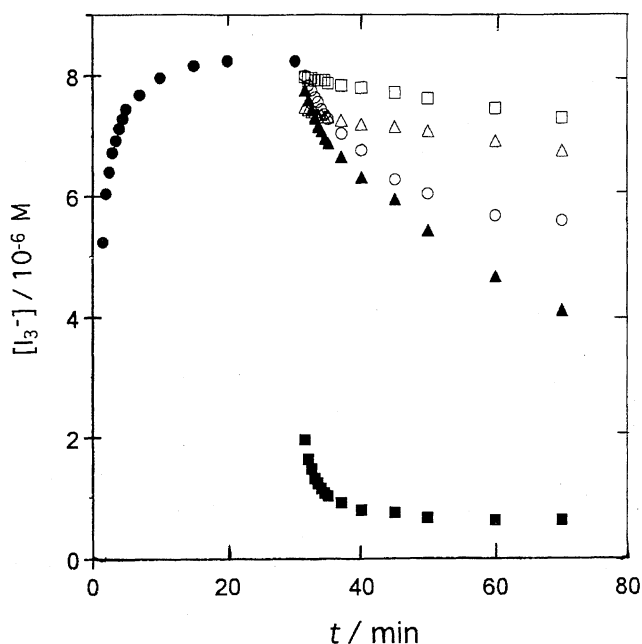
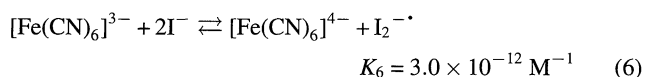
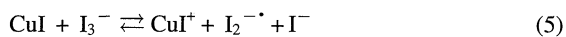
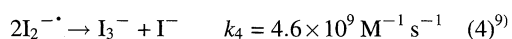
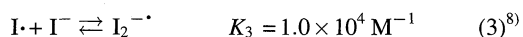
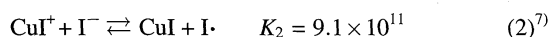
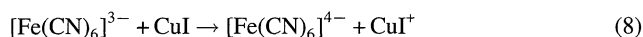
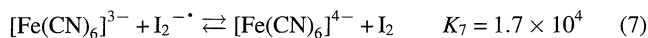
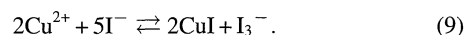


Fig. 7. Effect of the radical scavengers.

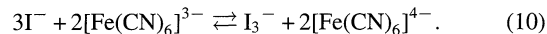
The plots \bullet indicate the I_3^- formation by the reaction between Cu^{2+} (2.0×10^{-5} M) and I^- (0.10 M) under conditions of N_2 -saturated at pH 3.8 (0.05 M CH_3COOH –0.01 M CH_3COONa) and 25 °C. Plots \square , \triangle , \circ , \blacktriangle , and \blacksquare indicate the cases that 1.6×10^{-5} M of acrylonitrile, acrylamide, oxalate, EDTA, or $[\text{Fe}(\text{CN})_6]^{4-}$ was, respectively, added at 30 min to the reacted solution indicated by the plots \bullet .



The equilibrium constants, K_6 and K_7 , were estimated from the E° values in Eqs. 13, 16, and 17. The plots using \bullet in Figs. 2, 3A, 5, and 7 are due to reactions (1)–(4), indicating an overall reaction of

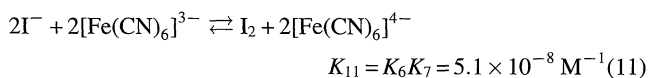


Reaction (9) is the same as $2\text{Cu}^{2+} + 4\text{I}^- \rightleftharpoons 2\text{CuI} + \text{I}_2$ plus $\text{I}_2 + \text{I}^- \rightleftharpoons \text{I}_3^-$ in reaction (C). The overall reaction (10) corresponding to the plots after 30 min in both Figs. 2 and 3A can be derived from either (2) + (3) + (4) + (5) + (6) + (7) + (C) or 2(2) + 2(3) + (4) + 2(8):

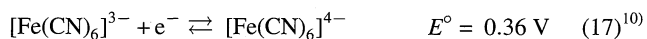


Either occurrence in directions of the reversible reaction (10), i.e., either $\{(2) + (3) + (4) + (5) + (6) + (7) + (C)\}$ or $\{2(2) + 2(3) + (4) + 2(8)\}$ is dependent on not only the concentrations of $[\text{Fe}(\text{CN})_6]^{3-}$ and $[\text{Fe}(\text{CN})_6]^{4-}$, but also on the pH in the reacting solutions. These consequences are revealed in Figs. 2, 3, and 5. If reactions (2), (3), (4), and (8) could occur predominantly, a quantitative increase of I_3^- should be observed in accordance with the forward reaction in Eq. 10. Such a tendency was found to exist in the rapid formation of I_3^- at $t \leq 2$ min in Fig. 2. However, such a behavior was not found at all in the plots after 30 min, at which

time $[Fe(CN)_6]^{3-}$ was added (see Fig. 2); on the contrary, a quantitative decrease in I_3^- was found in the case of having added $[Fe(CN)_6]^{4-}$ at 30 min (see Fig. 3A), indicating that the backward reaction rates in Eqs. 6 and 7 were much faster than their forward ones, and occurred together with all reactions of Eq. 2 to Eq. 7, and that the backward reaction in Eq. 10 occurred predominantly. Accordingly, in the case of having added $[Fe(CN)_6]^{3-}$ at 30 min, as given in Figs. 2 and 5A, reactions (2)–(7), after the occurrence of reaction (8), could operate to form I_3^- through competing with each other in the directions of the reversible reaction (10). Although the oxidation of I^- by $[Fe(CN)_6]^{3-}$, i.e., the forward reaction in Eq. 6 was found in the case of the HNO_2/I^- system in Fig. 6, such an oxidation reaction was not observed in the Cu^{2+}/I^- system given in Table 1 and the plots at $t \geq 40$ min in Figs. 2 and 5A. This also indicates that the backward reaction in Eq. 10 occurred dominantly in a whole reaction being composed of Eqs. 2, 3, 4, 5, 6, 7, and 8, and that the rate in Eq. 8 is much faster than that in the forward reaction of Eq. 6. It is noted herein that reaction (10) is essentially the same as Eq. 11, which can be derived from (6)+(7). Therefore, reactions (10) and (11) are thermodynamically one-sided to the left-hand side. It is also noted that Eqs. 10 and 11 are made up under any conditions in the presence and/or absence of Eq. 8, and that reaction (8) competes with both of the forward reactions in Eqs. 5 and 6, where there is probably a relationship of $k_5 > k_8$, judging from 0.54 V in Eq. 14 and 0.36 V in Eq. 17. Consequently, a kinetic behavior due to the constitution of Eq. 10 through reactions (2) to (4) with (8) was observed only under two conditions; $t \leq 2$ min in Fig. 2, in which reaction (5) could scarcely occur; also, when $[Fe(CN)_6]^{3-}$ was added to the reacted mixture of Cu^{2+} with I^- , the reaction (8) was apparently so negligible as to be seen in plots at $t \geq 40$ min in Figs. 2 and 5A.



All of the reactions written above are possible to occur from considering the following redox potentials:



Judging from the values of K_6 and K_7 , which were estimated by the above E° values, it is expected that the rate in the backward reaction of Eq. 6 is much faster than that in the forward one of Eq. 7. The value of k_{-6} can be evaluated to be $2.0 \times 10^9 \text{ M}^{-1} \text{ s}^{-1}$ by the relationship $K_6 = k_6/k_{-6}$, in which $k_6 = 6.1 \times 10^{-3} \text{ M}^{-2} \text{ s}^{-1}$ at pH 7.13 and 25 °C (Ref. 14). The fast occurrence of the backward reaction in Eq. 6, i.e.,

the oxidation reaction of $[Fe(CN)_6]^{4-}$ by $I_2^{\cdot-}$, was verified by Figs. 6 and 7, and the slowness of the forward reaction in Eq. 6 was verified by Fig. 2, inset. Accordingly, the reversible reaction (10) in the case of the CuI/CuI^+ catalysis could be extremely one-sided to the left-hand side. These are accounted for by the results shown in Figs. 2 and 3A. The quantitative decrease of I_3^- due to the added $[Fe(CN)_6]^{4-}$ (Table 1 and Fig. 3A) indicates that the forward reactions in both Eqs. 6 and 7 are negligible, or much slower, than their backward rates under the conditions of relatively large pH's. However, under the conditions of lower pH's, the I_3^- concentration decreased once, and then began to increase (see Fig. 5B), indicating that the rates of the forward reactions in Eqs. 6 and 7 are comparable to their backward ones under such conditions.

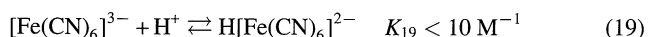
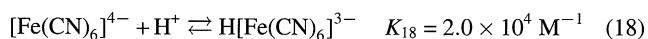
It is noted that the presence of the reversible reaction (5) plays an important role in making a catalytic reaction for reaction (10), and that reaction (5) essentially comprises reactions (2), (3), and (4). The concentrations of CuI^+ and $I_2^{\cdot-}$ in the equilibrium states of reactions (1) to (5) should be extremely low, because the CuI species is much more stable than the CuI^+ species, and the reactions (2) and (5) are extremely one-sided to the right- and left-hand side, respectively.

The steady states' concentration for the $I_2^{\cdot-}$ species in Eqs. 2, 3, 4, and 5 at the time to add $[Fe(CN)_6]^{4-}$ can be derived as $[I_2^{\cdot-}] = (k_5/k_4)^{1/2}([CuI][I_3^-])^{1/2}$, where $[CuI] = 2[I_3^-]$, and is thus dependent on the formed I_3^- concentrations with values of k_4 and k_5 . After the addition of $[Fe(CN)_6]^{4-}$, the radical anion $I_2^{\cdot-}$ decreased due to the occurrence of the backward reaction in Eq. 6 together with reaction (5), being followed by the rate equation of $-d[I_2^{\cdot-}]/dt = -d[I_3^-]/dt = 2^{1/2}k_{-6}(k_5/k_4)^{1/2}[I_3^-][Fe(CN)_6]^{4-}$. This relationship was verified by Fig. 4, in which the plots of $V_1 (= \Delta[I_3^-]_i/\Delta t)$ vs. $[I_3^-]_{t=30}$ were rectilinear under the conditions of a constant concentration of $[Fe(CN)_6]^{4-}$ with changing the added concentrations of Cu^{2+} (see Fig. 4, inset).

The quantitative decrease of I_3^- due to the added $[Fe(CN)_6]^{4-}$ (Table 1 and Fig. 3A) indicates that the forward reaction in Eqs. 7 and 8 are negligible, and that the backward reaction in Eq. 6 is much faster than the forward reaction in Eq. 7, i.e., $k_{-6} \gg k_7$. Further, the plots in all curves in Fig. 3A remained constant at ca. 60 min, showing the backward reaction rate in Eq. 6 as well as the forward reaction rate in Eq. 5 must be rapid. Because the value of E° in Eq. 14 is larger than that in Eq. 17, the relationship $k_5 \gg k_8$ is probable under conditions given in Table 1 and Fig. 3A.

Effect of the pH. Although the reaction of Cu^{2+} with I^- was not at all affected by the pH at the range 1.9–4.3, the catalyzed reaction after having added $[Fe(CN)_6]^{3-}$ and $[Fe(CN)_6]^{4-}$ was greatly affected by the pH values of the reacting solution. Namely, the I_3^- formation reaction by $[Fe(CN)_6]^{3-}$ was accelerated upon decreasing the pH (Fig. 5A); on the contrary, its decrease by $[Fe(CN)_6]^{4-}$ was retarded upon decreasing the pH (Fig. 5B). This is accounted for by the redox-potential increase in Eq. 17, which is caused by the much greater protonation for $[Fe(CN)_6]^{4-}$ than that for

$[\text{Fe}(\text{CN})_6]^{3-}$ (see Eqs. 18 and 19 with the relationship of $K_{18} \gg K_{19}$).¹⁵⁾



Accordingly, the forward reaction rates in Eqs. 6, 7, and 8 would be accelerated with decreasing pH, and on the contrary, their backward ones would be retarded. These considerations are in agreement with the results obtained given in Fig. 5.

In the case of the lower pH in Fig. 5B, the decrease in the I_3^- concentrations was not necessarily stoichiometric against the added $[\text{Fe}(\text{CN})_6]^{4-}$ concentrations (see plots \blacktriangle and \blacksquare in Fig. 5B), and the I_3^- concentrations began to gradually increase after they decreased once. This indicates that there are competing reactions in Eqs. 6, 7, and 8, and that the reversible reaction in Eq. 10 operates as an overall reaction.

Oscillation Reaction: The forward reaction rate in Eqs. 6, 7, and 8 competes with the backward ones in Eqs. 6 and 7. The increase of I_3^- is due to reactions (2), (3), (4), and (8), and its decrease is due to other reactions of Eqs. 2, 3, and 5 together with the backward reactions in Eqs. 6 and 7. Namely, there are not only some competitive reactions, but also two different paths in order to constitute an overall reaction (10). The obvious competition for the formation and reduction of I_3^- , being due to either directions' occurrence in the reversible reaction (10), i.e., either $\{(2) + (3) + (4) + (5) + (6) + (7) + (\text{C})\}$ or $\{2(2) + 2(3) + (4) + 2(8)\}$, could be seen among the plots \circ , \triangle , and \square in Fig. 2; the lowest concentration of the added $[\text{Fe}(\text{CN})_6]^{3-}$, i.e., the plots indicated by \circ are much larger than those by \triangle at $t \leq 20$ min, and are only slightly larger or almost equivalent at $t > 30$ min, and the plots indicated by \square are much larger than those by \triangle . Such a competitive-reaction situation might have led to fluctuation plots like an oscillating reaction at $t \geq 30$ min in Figs. 2 and 5A.

On the Ion-Pair between Cu^{2+} and $[\text{Fe}(\text{CN})_6]^{3-}$ or $[\text{Fe}(\text{CN})_6]^{4-}$. When a solution of $\text{K}_3[\text{Fe}(\text{CN})_6] \geq 2.0 \times 10^{-4}$ M or $\text{K}_4[\text{Fe}(\text{CN})_6] \geq 5.0 \times 10^{-5}$ M was mixed with 4.0×10^{-4} M CuSO_4 , a white or brown turbidity (sediment) was found in the solution, respectively. However, no precip-

itations were found under the conditions of 0.10 M KI, CuSO_4 (3.5×10^{-6} — 2.0×10^{-5} M), and $[\text{Fe}(\text{CN})_6]^{4-/3-}$ (5.0×10^{-7} — 2.0×10^{-5} M) in this work. Since about 80% copper(II) ion in the present study becomes CuI with a large stability (refer to Eq. 2), it should be unfavorable for making the ion-pair between Cu^{2+} and $[\text{Fe}(\text{CN})_6]^{4-/3-}$. Accordingly, the ion-pair species' formation must be negligible. However, a slight and rapid decrease in I_3^- at the initial stage of the $[\text{Fe}(\text{CN})_6]^{3-}$ addition at 30 min in Figs. 2 and 5A might arise from a slight formation of $\{\text{Cu}_2^{4+} \cdot [\text{Fe}(\text{CN})_6]^{4-}\}$, which could induce an occurrence of all reverse reactions in Eqs. 1, 2, and 3 with the forward reaction in Eq. 5.

References

- 1) M. Kimura, Y. Shiga, and K. Tsukahara, *Bull. Chem. Soc. Jpn.*, **71**, 2345 (1998).
- 2) M. Kimura, R. Ikawa, Y. Shiota, and K. Tsukahara, *Bull. Chem. Soc. Jpn.*, **71**, 893 (1998).
- 3) M. F. Ruasse, J. Aubard, B. Gallard, and A. Adenier, *J. Phys. Chem.*, **90**, 4382 (1986).
- 4) A. D. Awtrey and R. E. Connick, *J. Am. Chem. Soc.*, **73**, 1842 (1986).
- 5) M. Kimura, H. Ishiguro, and K. Tsukahara, *J. Phys. Chem.*, **94**, 4106 (1990).
- 6) M. Kimura, M. Sato, T. Murase, and K. Tsukahara, *Bull. Chem. Soc. Jpn.*, **66**, 2900 (1993).
- 7) M. Kimura, A. Ohomura, F. Nakazawa, and K. Tsukahara, *Bull. Chem. Soc. Jpn.*, **64**, 1872 (1991).
- 8) M. Kimura, F. Nakazawa, and K. Tsukahara, *Bull. Chem. Soc. Jpn.*, **65**, 1812 (1992).
- 9) L. I. Grossweiner and M. S. Matheson, *J. Phys. Chem.*, **61**, 1089 (1959).
- 10) W. M. Latimer, "The Oxidation States of the Elements and Their Potentials in Aqueous Solutions," 2nd ed, Prentice-Hall, New York (1952).
- 11) A. Barkatt and M. Ottolenghi, *Mol. Photochem.*, **6**, 253 (1974).
- 12) A. Haim and H. Taube, *J. Am. Chem. Soc.*, **85**, 495 (1963).
- 13) W. H. Woodruff and D. W. Margerum, *Inorg. Chem.*, **12**, 962 (1973).
- 14) W. L. Reynolds, *J. Am. Chem. Soc.*, **80**, 1830 (1958).
- 15) "Kagaku Binran, Kisohehen II," (in Japanese), ed by Chemical Society of Japan, Maruzen, Tokyo (1984), p. 473.